Published in final edited form as:

J Cataract Refract Surg. 2016 February ; 42(2): 284–295. doi:10.1016/j.jcrs.2015.09.021.

Subclinical keratoconus detection by pattern analysis of corneal and epithelial thickness maps with optical coherence tomography

Yan Li, PhD, **Winston Chamberlain, MD, PhD**, **Ou Tan, PhD**, **Robert Brass, MD**, **Jack L. Weiss, MD**, and **David Huang, MD, PhD**

Center for Ophthalmic Optics and Lasers (Li, Chamberlain, Tan, Huang), Casey Eye Institute and Department of Ophthalmology, Oregon Health and Science University, Portland, Oregon, the Brass Eye Center (Brass), Latham, New York, and the Gordon Weiss Schanzlin Vision Institute (Weiss), San Diego, California, USA.

Abstract

PURPOSE—To screen for subclinical keratoconus by analyzing corneal, epithelial, and stromal thickness map patterns with Fourier-domain optical coherence tomography (OCT).

SETTING—Four centers in the United States.

DESIGN—Cross-sectional observational study.

METHODS—Eyes of normal subjects, subclinical keratoconus eyes, and the topographically normal eye of a unilateral keratoconus patient were studied. Corneas were scanned using a 26 000 Hz Fourier-domain OCT system (RTVue). Normal subjects were divided into training and evaluation groups. Corneal, epithelial, and stromal thickness maps and derived diagnostic indices, including pattern standard deviation (PSD) variables and pachymetric map–based keratoconus risk scores were calculated from the OCT data. Area under the receiver operating characteristic curve (AUC) analysis was used to evaluate the diagnostic accuracy of the indices.

RESULTS—The study comprised 150 eyes of 83 normal subjects, 50 subclinical keratoconus eyes of 32 patients, and 1 topographically normal eye of a unilateral keratoconus patient. Subclinical keratoconus was characterized by inferotemporal thinning of the cornea, epithelium,

Corresponding author: Yan Li, PhD, Casey Eye Institute, Oregon Health and Science University, 3375 Southwest Terwilliger Boulevard, Portland, Oregon, USA 97239. liyan@ohsu.edu.

Presented in part at the ASCRS Symposium on Cataract, IOL and Refractive Surgery, San Francisco, California, April 2013, and the annual meeting of the Association for Research in Vision and Ophthalmology, Seattle, Washington, USA, May 2013.

Financial disclosures: Oregon Health and Science University and Drs. Li, Tan, and Huang have a significant financial interest in Optovue, Inc. Dr. Brass receives research grants from Optovue, Inc. Drs. Chamberlain and Weiss have no financial or proprietary interest in any material or method mentioned.

Pattern analysis performed on corneal and epithelial thickness maps measured by Fourier-domain OCT showed that corneal and epithelial pattern standard deviation variables detected subclinical keratoconus with high accuracy.

and stroma. The PSD values for corneal ($P < .001$), epithelial ($P < .001$), and stromal ($P = .049$) thickness maps were all significantly higher in subclinical keratoconic eyes than in the normal group. The diagnostic accuracy was significantly higher for PSD variables (pachymetric PSD, AUC = 0.941; epithelial PSD, AUC = 0.985; stromal PSD, AUC = 0.924) than for the pachymetric map–based keratoconus risk score (AUC = 0.735).

CONCLUSIONS—High-resolution Fourier-domain OCT could map corneal, epithelial, and stromal thicknesses. Corneal and sublayer thickness changes in subclinical keratoconus could be detected with high accuracy using PSD variables. These new diagnostic variables might be useful in the detection of early keratoconus.

Unrecognized early-stage keratoconus is the leading cause of iatrogenic ectasia after laser in situ keratomileusis (LASIK) and remains the major challenge of preoperative refractive surgery screening.[1–6] Moreover, the early detection of keratoconus could assist in decision-making situations, such as when assessing the need for early intervention with corneal collagen crosslinking treatments.[7,8] Corneal topography is currently the gold standard to evaluate ectatic corneal disorders such as keratoconus and pellucid marginal degeneration (PMD).[9–13] Normal, suspicious, or abnormal topography patterns of these diseases have been classified. However, clinicians report eyes with normal topography and no other known risk factors that still developed post-LASIK keratectasia.[6,14,15] It is likely that corneal topography does not capture all cases at risk. More recently, researchers found that the corneal epithelium remodels in response to underlying stromal irregularities.[16–18] Therefore, analyzing the corneal epithelium and stroma separately might provide additional information for the diagnosis of keratoconus.[18–22]

Optical coherence tomography (OCT) is a noncontact technique that is based on the principles of low-coherence interferometry.[23] The high axial resolution allows precise delineation of corneal surfaces. Previously, we showed that OCT can provide accurate pachymetry (corneal thickness) and corneal epithelial thickness maps.[21,24–26] We also found that keratoconus can be detected by abnormal corneal thinning and characterized by apical epithelial thinning. In this study, we performed pattern analysis on pachymetric, corneal epithelial, and stromal thickness maps in eyes with subclinical keratoconus and in normal eyes to facilitate the early detection of keratoconus.

SUBJECTS AND METHODS

Subjects in this cross-sectional observational study were recruited at Doheny Eye Institute at the University of Southern California (USC), Los Angeles, California; the Brass Eye Center, Latham, New York; the Gordon Weiss Schanzlin Vision Institute, San Diego, California; and the Casey Eye Institute at Oregon Health and Science University (OHSU), Portland, Oregon. The study followed the tenets of the Declaration of Helsinki and was in accord with the U.S. Health Insurance Portability and Accountability Act of 1996. The institutional review boards (IRBs) of USC and OHSU and the Western IRB (Olympia, Washington, USA) approved the study protocol. Clinical trial registration was not required because of the observational nature of the study. All subjects were at least 18 year old, and all provided written informed consent.

Normal subjects were recruited from volunteers and patients seeking refractive surgery or cataract surgery consultation. All had normal slitlamp microscopy and normal topography. Normal subjects were divided into a training group and an evaluation group for data-analysis purposes. The subclinical keratoconic eyes included in this study satisfied the following clinical and topographic criteria: no slitlamp findings, corrected distance visual acuity (CDVA) of 20/20 or better, and the presence of asymmetric bowtie with a skewed radial axis, central or inferior steepening, or a claw-shape pattern on topography.[27–29] In addition, a forme fruste keratoconus[30] case that was the topographically normal eye of a unilateral keratoconus patient was included in this study. None of the eyes had signs or a history of other corneal disease, and none had previous refractive or other ocular surgery.

Optical Coherence Tomography

A Fourier-domain OCT system (RTVue, Optovue, Inc.) with a corneal adaptor module was used. The OCT system has a working wavelength of 830 nm and operates at a scan speed of 26 000 axial scans per second. It has a depth resolution of 5 μm (full-width–half-maximum) in tissue. The wide-angle (corneal long) adaptor lens used in this study provides a 6.0 mm long scan width. A “Pachymetry+Cpwr” scan pattern (6.0 mm scan diameter, 8 radials, 1024 axial scans each, repeated 5 times) centered at the pupil center was used to map the cornea (Figure 1). Each eye was scanned 2 or 3 times during a single visit. Subjects were repositioned after each OCT scan.

Fourier-domain OCT image data were exported and processed with purpose-designed software (Matlab, version 7.10, the Mathworks, Inc.). The air–tear interface, epithelium–Bowman layer, and posterior corneal boundaries were automatically identified with software algorithms.[A] Corneal OCT images were dewarped to remove the distortion caused by light refraction at the interface and transition in the tissue.[25,31] Corneal thickness was measured as the distance between the air–tear and cornea–aqueous interfaces. Corneal epithelial thickness was measured as the distance between the air–tear and the epithelium–Bowman interfaces. Both thicknesses were acquired perpendicular to the anterior surface at the point of measurement. Corneal stromal thickness was calculated by subtracting the epithelial thickness from the corneal thickness. Thickness profiles were generated from each meridional cross-section.

Six-millimeter diameter corneal and epithelial thickness maps were generated by interpolating corneal and epithelial thickness meridional profiles, respectively. The stromal thickness map was calculated by subtracting the epithelial thickness map from the corneal thickness map. The minimum epithelial, corneal, and stromal thicknesses inside the central 5.0 mm diameter area were recorded.

The study used a previously developed a pachymetric map–based keratoconus risk score for keratoconus detection.[32] The risk score is a summation of 5 component scores derived from 5 pachymetric variables: the minimum, minimum–median, superior–inferior, superonasal–inferotemporal, and vertical location of the thinnest cornea. A component variable would have a score of 1, 2, or 3 if its value exceeded the 20th, 5th, or 1st percentile measurements in normal subjects. An OCT pachymetry map–based keratoconus evaluation table was developed to record this risk score[32] (worksheet available at the Center for Ophthalmic

Optics and Lasers website[B]). This score was presented for comparison with newer diagnostic variables introduced in this paper.

Pattern Standard Deviation Variables

Pachymetric, epithelial, and stromal pattern standard deviation (PSD) variables were calculated using the central 5.0 mm diameter pachymetric, epithelial, and stromal thickness maps.

Pattern Deviation Maps

Pattern deviation maps were generated to evaluate the difference between an individual pattern map and the average pattern map of normal subjects. The pattern deviation maps were designed to highlight abnormal thickness patterns. Zero or near zero pattern deviation values indicate normal thickness pattern and are shown in green. Negative pattern deviation values indicate relative thinning compared with the normal values and are shown in blue or purple. Positive pattern deviation values indicate relative thickening and are shown in yellow or red.

Below, the epithelial pattern deviation map (PD_E) is used as an example to describe the process step-by-step.

First, the epithelial pattern map of the normal reference population P_{NE} was calculated by

$$P_{NE}(x,y)=T_{NE}(x,y)/\overline{T_{NE}} \quad (1)$$

where T_{NE} is the average epithelial thickness map of all normal subjects in the training group and $\overline{T_{NE}}$ is the average thickness of map T_{NE}.

The individual epithelial pattern map P_E was calculated as

$$P_E(x,y)=T_E(x,y)/\overline{T_E} \quad (2)$$

where T_E is the individual epithelial thickness map and $\overline{T_E}$ is the average thickness of the map.

Next, the epithelial pattern deviation map (PD_E) was calculated by subtracting the average normal epithelial pattern map (P_{NE}) from the individual epithelial pattern map (P_E) as follows:

$$PD_E(x,y)=P_E(x,y)-P_{NE}(x,y) \quad (3)$$

Similarly, the pachymetric (corneal thickness) pattern map (PD_P) and stromal pattern map (PD_S) were calculated using pachymetry maps and stromal thickness maps.

Pattern Standard Deviation Variables

Furthermore, the epithelial thickness map PSD ($PSD_{E)}$ variable was calculated from the epithelial pattern deviation map as

$$\mathrm{PSD}_E = \sqrt{\frac{\sum_x \sum_y (\mathrm{PD}_E(x,y))^2}{N}} \quad (4)$$

where $PD_E(x,y)$ is the epithelial pattern deviation value at map location (x,y) and N is the total number of the map points inside the analytic zone (central 5.0 mm diameter).

The pachymetric PSD variable (PSD_P) and stromal PSD variable (PSD_S) were calculated in a similar manner.

Topography

Corneal topography was obtained using the Orbscan II (Bausch & Lomb) or Pentacam (Oculus Surgical, Inc.) for all study subjects. The steep keratometry (K) reading of the simulated K reading was recorded. The topography-based keratoconus percentage index (KISA%)[12] was calculated for subjects recruited at the OHSU site.

Statistical Analysis

Normal subjects older than 65 years were excluded from data analysis to match the age of the subclinical keratoconus group. Descriptive statistics and other statistical analyses including *t* tests were performed using Medcalc 12.0 software (Medcalc Software bvba). Mean ± standard deviation (SD) values of the minimum thickness, pachymetric map– based keratoconus risk score, and PSD variables were calculated for the normal group and the subclinical keratoconus group. The repeatability of PSD variables was assessed by the intraclass correlation (ICC) and pooled SD obtained from the multiple measurements of each eye. Measurements from repeated scans were averaged for each eye for statistical analysis except for the repeatability evaluation. The normality of the variables was confirmed by a Kolmogorov-Smirnov test on the dataset from which 1 eye was randomly selected from each normal subject.

To compare PSD variables and the pachymetric map–based keratoconus risk score measured in normal eyes and subclinical keratoconic eyes, 2-tailed *t* tests were performed. If both eyes of a subject were involved in the study, a randomly selected eye was chosen for the *t* test to avoid the correlation between the 2 eyes of the same patient. A *P* value less than 0.05 was considered statistically significant.

Receiver operating characteristic (ROC) curve analyses were performed to evaluate the diagnostic performance of the PSD variables and the pachymetric map–based keratoconus risk score. Normal subjects in the evaluation group and all subclinical keratoconic subjects were involved in the ROC curve analyses. If both eyes of a subject were involved in the study, a randomly selected eye was chosen for the ROC curve analyses. The area under ROC curve (AUC) was calculated for each variable. The diagnostic power of the variables was compared by the area under different ROC curves. A cutoff value of each variable was selected with the highest average of sensitivity and specificity. Corresponding sensitivity and specificity values were recorded. Venn diagrams were used to illustrate the overlap between abnormal PSD measurements in normal eyes and subclinical keratoconus eyes. To assess the

diagnostic power of the OCT-based PSD variables in subclinical keratoconus patients with a normal topographic KISA% index, separate ROC curve analyses were performed for OHSU subjects with KISA% measurements less than 60.

The pachymetric, epithelial, and stromal PSD cutoff values obtained in the ROC analysis were used to evaluate the abnormality of the forme fruste keratoconic cornea.

RESULTS

Data were analyzed for 150 eyes of 83 normal subjects (38 men, 45 women), 50 subclinical keratoconic eyes of 32 patients (17 men, 15 women), and the topographically normal eye of a unilateral keratoconus patient (right eye of a 22-year-old man). The mean age was 47.2 years ± 14.1 (SD) (range 19 to 65 years) in normal subjects and 42.7 ± 14.5 years (range 20 to 63 years) in subclinical keratoconus patients ($P = .093$). Table 1 shows the steep K, visual acuity, minimum pachymetry, epithelial, and stromal thicknesses readings.

Fifty normal eyes (32 subjects) matching the number of subclinical keratoconus cases were assigned to the evaluation group. The remaining 100 normal eyes (51 subjects) were assigned to the training group for calculating the population average normal pachymetric, epithelial, and stromal thickness maps (T_{NP}, T_{NE}, and T_{NS}) and the average normal pachymetric, epithelial, and stromal pattern maps (P_{NP}, P_{NE}, and P_{NS}).

Figure 2 shows the group average thickness maps. The thinnest points on the average pachymetric and stromal thickness maps were slightly inferotemporal to the center. The average subclinical keratoconic eye showed general thinning and focal inferotemporal thinning compared with the normal average eye. The epithelial thickness maps showed different patterns. The average normal epithelial thickness map was thickest at the center and thinner superiorly. In contrast, the average subclinical keratoconic eye showed inferotemporal epithelial thinning and superonasal thickening.

Figure 3 shows the pachymetric, epithelial, and stromal pattern deviation maps and topography maps of 1 normal eye and 2 subclinical keratoconus eyes. In a typical subclinical keratoconic eye (CDVA 20/20), the epithelial pattern deviation map (Figure 3, *f*) showed inferotemporal thinning and relative superior thickening and the pachymetric (Figure 3, *e*) and stromal (Figure 3, *g*) pattern deviation maps also showed focal thinning. In a very subtle subclinical keratoconic eye (CDVA 20/15); the epithelial pattern deviation map (Figure 3, *j*) again showed inferotemporal thinning and relative superior thickening, but the pachymetric (Figure 3, *i*) and stromal (Figure 3, *k*) pattern deviation maps did not show a significant variation that could be distinguished from the relatively uniform normal pattern deviation maps (Figure 3, *a* to *c*).

Figure 4 shows the average pachymetric, corneal epithelial, and stromal pattern deviation maps of subclinical keratoconic eyes. The average epithelial pattern deviation map (Figure 4, *b*) in the subclinical keratoconus group showed marked inferotemporal thinning and relative thickening in the surrounding area. The average pachymetric map and stromal pattern deviation maps (Figure 4, *a* and *c*, respectively) also showed focal inferotemporal thinning;

however, the location was slightly more inferior than temporal and the degree of relative thinning was not as significant as on the epithelial pattern deviation map.

Compared with normal eyes, subclinical keratoconic eyes had significantly higher PSD measurements and pachymetric map–based risk scores (Table 2). The epithelial PSD provided the cleanest separation between the subclinical keratoconic eyes and the normal eyes, with the least overlap in distribution (Table 2 and Figure 5). Analysis of the Venn diagrams showed that epithelial PSD identified the most abnormal cases in the subclinical keratoconic group and did not misidentify any abnormality in the normal group (Figure 6). Epithelial PSD had the highest diagnostic power (AUC = 0.985; sensitivity = 96.0%; specificity = 100% (Table 3). The pachymetric and stromal PSD variables also gave very good diagnostic power (AUC = 0.941 and AUC = 0.924, respectively). No statistically significant difference was found between the AUC of the pachymetric, epithelial, and stromal PSD variables ($P > .09$). In comparison, the diagnostic accuracy of the pachymetric map–based keratoconus risk score was significantly lower (AUC = 0.735; $P < .0001$).

Topography-based KISA% index measurements were obtained in 24 eyes of 19 subjects with subclinical keratoconus and 36 eyes of 19 normal subjects recruited at the OHSU site. Twenty eyes of 14 subjects with subclinical keratoconus and all normal eyes had normal KISA% values (<60%). The diagnostic power of the PSD variables for subclinical keratoconus with a normal KISA% remained very good (pachymetric PSD, AUC = 0.943 and sensitivity = 82.4%; epithelial PSD, AUC = 0.961 and sensitivity = 88.9%; stromal PSD, AUC = 0.90 and sensitivity = 84.2%).

The repeatability of PSD variables was good based on ICC values (0.836 to 0.982) and pooled SD values (0.0018 to 0.0033) (Table 4). The epithelial PSD had the highest ICC values in both the normal group and subclinical keratoconus group. The pooled SD values were smaller than to the average subclinical keratoconus PSD measurements, with the ratio being 8.1% for the pachymetric PSD, 4.1% for the epithelial PSD, and 9.6% the stromal PSD. Again, the epithelial PSD was the most repeatable as judged by this ratio.

Noticeably, in the topographically normal eye of the unilateral keratoconus case (Figure 3, *m* to *p*) (CDVA 20/15), the epithelial pattern deviation map (Figure 3, *n*) showed an abnormal pattern of epithelial thinning inferiorly and thickening superiorly. However, the topography map (Figure 3, *p*) and the pachymetric and stromal pattern deviation maps (Figure 3, *m* and *o*, respectively) all appeared normal. The epithelial PSD measurement was abnormal (0.057). The pachymetric and stromal PSD values were in normal range (0.012 and 0.010, respectively).

DISCUSSION

In this study, we found that corneal PSD variables could accurately detect characteristic corneal, stromal, and epithelial thickness changes in eye with subclinical keratoconus.

Keratoconus is a noninflammatory ectatic disease characterized by progressive thinning and apical protrusion.[33] Unidentified early stage keratoconus is the primary risk factor for post-LASIK ectasia, a serious complication of this common vision-correction procedure. Current

detection of subclinical keratoconus relies primarily on corneal topography. However, topography may not capture all cases at risk because cases with normal preoperative topographies but that developed ectasia after laser vision correction were reported by Randleman et al.,[6] Ambrósio et al.,[14] Klein et al.,[15] and others. One possible reason is that topography measures anterior topographic distortion only. However, keratoconus could also be characterized by posterior topographic steepening, focal corneal thinning, or focal epithelial thickness variation. In early keratoconus, focal steepening at the apex tends to be covered up by compensatory corneal epithelial thinning.[18,21,34,35] Thus detecting focal epithelial thinning may be a more sensitive way of identifying keratoconus in its very early stage.

Many different terms (eg, *keratoconus suspect, subclinical keratoconus, forme fruste keratoconus, early keratoconus, borderline keratoconus*) have been used in medical literature to describe very early preclinical stage of keratoconus.[30,36] In this study, we followed the keratoconus grading scheme suggested by the Collaborative Longitudinal Evaluation of Keratoconus Study group.[18] The term *subclinical keratoconus* used in this paper refers to corneas with a topographic pattern consistent with early keratoconus but no clinical signs of keratoconus and with normal spectacle acuity (CDVA 20/20 or better).[18,37,38] Moreover, the term *forme fruste keratoconus* in this study corresponds to the topographically normal eye that has keratoconus in the fellow eye.[30,39]

Optical coherence tomography, very-high-frequency (VHF) ultrasound (US) biomicroscopy, scanning-slit corneal technology, and the rotating Scheimpflug camera have enabled analysis of corneal thickness and posterior corneal curvature. Corneal thinning is a key pathologic feature of keratoconus. Many research groups, including Reinstein et al.,[34] Rabinowitz et al.,[40] and Pflugfelder et al.,[41] report that keratoconic corneas were significantly thinner than normal corneas. In our previous studies,[24,32] we used OCT pachymetric-based variables for keratoconus screening and yielded high diagnostic power, with AUC values of 0.975 to 0.99. Ambrósio et al.[42] introduced various Scheimpflug system-based pachymetric variables to differentiate between normal corneas and keratoconic corneas and yielded an AUC of 0.987. More recently, Reinstein et al.[34] used VHF US to measure epithelial thickness profiles and maps and reported epithelial thinning over the cone location and thickening in the surrounding area in keratoconic eyes.[42,43] This keratoconic epithelial thickness pattern has been confirmed by several other studies.[18,20–22,43] In 2015, Temstet et al.[44] reported that epithelial thickness in the thinnest corneal zone could be used to diagnose forme fruste keratoconus but was not sufficient as the sole diagnostic index.

Our group first developed automatic methods to map corneal epithelium thickness with Fourier-domain OCT in normal eyes and keratoconic eyes.[21] We proposed several epithelial thickness–based variables for keratoconus detection and discovered that the epithelial PSD variable gave excellent diagnostic power, with an AUC of 1.00.[21] We further want to test the epithelial PSD variable on the more challenging problem of detecting subclinical keratoconus and forme fruste keratoconus. We also performed pattern analysis on pachymetric and stromal thickness maps to determine whether the PSD approach could improve their diagnostic performance in cases of subclinical keratoconus.

In this study, we found that the average subclinical keratoconic eye showed inferotemporal epithelial thinning and superonasal thickening. In contrast, the average normal epithelial thickness map was thickest at the center and thinner superiorly. The pachymetry and stromal thickness maps had different patterns; in general, average subclinical keratoconic eyes were thinner and had focal inferotemporal thinning than the average normal eye. These abnormal thickness patterns were highlighted more in the pattern deviation maps. The average epithelial pattern deviation map in the subclinical keratoconus group showed marked inferotemporal thinning and relative thickening in the surrounding area. The average pachymetric and stromal pattern deviation maps also showed focal inferotemporal thinning; however, the location was slightly more inferior than temporal and the degree of relative thinning was not as significant as on the epithelial pattern deviation map.

The repeatability of 3 PSD variables was adequate compared with the population average of subclinical keratoconic measurements. The epithelial PSD had the best ICC, and its SD of repeated measurement was better than that of the pachymetric PSD by about a factor of 2 when normalized to the PSD value in the subclinical keratoconus group. This indicates that the epithelial PSD has the best potential to be used for keratoconus diagnosis and staging.

Researchers have considered that the contralateral topographically normal eye of a patient with unilateral keratoconus might represent the mildest and earliest form of keratoconus (referred to as forme fruste keratoconus in the literature).[39] In this study, epithelial map pattern analysis (Figure 3, *n*) and the epithelial PSD variable detected abnormality in the topographically normal eye of a patient with unilateral keratoconus. This suggests that epithelial pattern analysis might have the capability to detect corneal ectatic abnormality earlier than topography. More forme fruste keratoconus cases are needed to validate this observation in future studies.

All 3 PSD variables had a diagnostic accuracy much higher than the pachymetric map–based keratoconus risk score (PSD variables AUC = 0.924 to 0.985 versus keratoconus risk score AUC = 0.735) ($P < .0001$). Among them, the epithelial PSD variable had the highest diagnostic power (AUC = 0.985) in subclinical keratoconus detection. The corneal epithelium plays an important smoothing role in reducing the irregularity of the anterior stromal surface in keratoconus.[17,34] The epithelium becomes thinner over the apex of the cone to reduce focal steepening. This focal thinning is more easily detectable in the epithelial map because the epithelium is much thinner than the entire corneal thickness. Assuming an epithelial thickness of 50 μm and a corneal thickness of 550 μm, 5 μm of thinning corresponds to a 10% change in the epithelial thickness but only a 1% change in pachymetry. This advantage was shown in our subclinical keratoconus group, which had a greater increase in the epithelial PSD than in the pachymetric and stromal PSDs. In addition to OCT, VHF US can measure a corneal epithelial thickness map and might benefit from the epithelial PSD for keratoconus screening.[34] The pachymetric PSD variable also provided good diagnostic power (AUC = 0.941). It is particularly interesting and useful because pachymetry maps are commonly available. Imaging modalities having sufficient resolution to map the corneal thickness but not the epithelial thicknesses, such as scanning-slit corneal technology and rotating Scheimpflug imaging, can also benefit from the pachymetry PSD variable for keratoconus detection. On the other hand, the stromal PSD variable neither

outperformed (lowest AUC among 3 PSD variables) nor added more information to the epithelial and pachymetric PSD variables, as shown in the Venn diagrams in Figure 6. Therefore, we recommend implementing the pachymetric and epithelial PSD variables only when using clinical instruments.

A literature review found various recent studies focused on the detection of early keratoconus. Several research groups used a scanning-slit tomographer or Scheimpflug camera to measure posterior corneal elevation for discriminating corneas with subclinical keratoconus from normal corneas.[45–48] Some recommended that posterior corneal elevation provided useful information but could not be used alone to identify eyes with subclinical keratoconus.[45,46] Saad and Gatinel[43] proposed a discriminant function using both corneal thickness and posterior corneal elevation measurements for identifying forme fruste keratoconus. Their discriminant function reached an AUC of 0.99. Wavefront technology has also been studied as a way to diagnose keratoconus. Bühren et al.[49] found that anterior corneal surface aberrations could be used for subclinical keratoconus detection in their innovative study. Later, they showed that data from a Zernike decomposition of the anterior and posterior corneal surfaces in conjunction with pachymetry data was useful for the detection of subclinical keratoconus.[37,50] Shetty et al.[51] performed Zernike analyses of corneal thickness maps and calculated the root mean square (RMS) of the difference between the measured corneal thickness and the Zernike analysis–interpolated corneal thickness maps. They found that the 2nd-order and 3rd-order RMS values of the performed Zernike analysis coefficients were the best predictors of keratoconic corneas. In their 2012 study, Saad and Gatinel[39] confirmed the usefulness of total and corneal wavefront higher-order aberrations for the detection of forme fruste keratoconus. Moreover, Arbelaez et al.[52] developed a new classification algorithm for the detection of subclinical keratoconus using a machine learning technique—the support vector machine—which is based on corneal measurements provided by a Scheimpflug camera combined with Placido corneal topography (Sirius, Costruzione Strumenti Oftalmici). The authors reported excellent results in a large data sample with 92.0% sensitivity and 97.7% specificity for detecting subclinical keratoconus. They showed that the use of the posterior surface and thickness parameters improved the sensitivity of subclinical keratoconus detection from 75.2% to 92.0%. Smadja et al.[53] used a machine learning classifier—the classification and regression tree—to differentiate between normal corneas and forme fruste keratoconus corneas with corneal measurements acquired by a dual Scheimpflug analyzer system (Galilei, Ziemer Ophthalmic Systems AG). Their study achieved 93.7% sensitivity and 97.2% specificity with the large tree discriminating rule and 90% sensitivity and 86% specificity with the pruned tree discriminating rule.[53] Their algorithm selected the posterior asphericity asymmetry index and the corneal volume to be the 2 most discriminant variables for differentiating between normal eyes and eyes with forme fruste keratoconus. Silverman et al.[18] proposed a neural network machine–based method using 161 features extracted from VHF US– generated corneal, epithelial, and stromal thickness maps and achieved a mean specificity of 99.5% ± 1.5% and a mean sensitivity of 98.9% ± 1.9% in identifying eyes with keratoconus from normal eyes. These are all promising approaches using different technologies. Our approach uses the high axial resolution of OCT and its capability of noncontact epithelial thickness

mapping to achieve high diagnostic accuracy. The methods are not directly comparable because of the different characteristics of the subjects evaluated.

Pattern standard deviation detects any deviation from the normal pattern. Thus, although we have shown that PSD is very accurate in detecting subclinical keratoconus in this study, we believe it would also detect other corneal abnormalities, such as dry eye, contact lens–induced warpage, previous keratorefractive surgery, epithelial basement membrane dystrophy, Salzmann nodular degeneration, corneal edema, and corneal scars. To establish a diagnosis of subclinical keratoconus, the clinician should use an abnormally high PSD as a starting point only; this should be corroborated by specific patterns of inferotemporal thinning and steepening on pachymetric, epithelial, and topographic maps. A clinical history is useful. For example, an eye with a history of myopic LASIK would be expected to have central topographic flattening, pachymetric thinning, and epithelial thickening.[17] The pachymetry-based keratoconus risk score is composed of 5 indices that characterize keratoconus. Although they are not as sensitive as the PSD, these other pachymetric indices could be useful in differential diagnosis. For example, a low minimum pachymetry is consistent with keratoconus; however, if it is above normal, additive pathologies (eg, epithelial basement membrane dystrophy, Salzmann nodular degeneration, or corneal edema) would be more likely to explain a high PSD. The location of the thinnest cornea is also informative. For example, in keratoconus the locations of corneal thinning and epithelial thinning on OCT thickness maps are usually inferotemporal and roughly consistent with the location of corneal steepening shown on the corneal topography map. In contrast, contact lens warpage would show flattening on the corneal topography where the epithelium is the thinnest. Thus, the primary role of pachymetry and the epithelial PSD parameters is to serve as very sensitive detectors of corneal shape abnormalities in general. The identification of the specific abnormality would still require the clinician to recognize the patterns on the OCT pachymetry and epithelial thickness maps and correlate them with corneal topography and clinical information.

One limitation of the technology used in this study was the limited 6.0 mm diameter size of the thickness maps. A larger map size will facilitate the comparison of the thickness map patterns for diseases involving more peripheral cornea, such as PMD. We will evaluate the PSD variables acquired with a larger map in future studies. Another limitation is that we did not have contact lens–wearing information for most study subjects except for the 20 subclinical keratoconic patients and 1 forme fruste keratoconic subject. The forme fruste keratoconic subject had no history of contact lens use. Of the 20 subclinical keratoconic subjects, 12 had no history of contact lens wear; 3 wore rigid gas-permeable contact lenses, but the last wearing was at least 2 months before the OCT examination; and 5 wore soft contact lens, but the last wearing was at least 1 week before the OCT examination. This deserves more attention in future studies.

In summary, high-resolution Fourier-domain OCT was capable of mapping corneal, epithelial, and stromal thicknesses. Characteristic corneal and its sublayer thickness changes in subclinical keratoconus could be detected with very high accuracy using PSD variables. These new diagnostic variables might be useful in the detection of early keratoconus.

Acknowledgments

Supported by the National Institutes of Health, Bethesda, Maryland (grant R01EY018184), a research grant from Optovue, Inc., Fremont, California, and an unrestricted grant to Casey Eye Institute from Research to Prevent Blindness, Inc., New York, New York, USA. The sponsor or funding organization had no role in the design or conduct of this research.

Dr. Qienyuan Zhou coordinated the study data collection, Dr. Xinbo Zhang provided statistics consultation, and Dr. Maolong Tang provided consultation on corneal topography.

REFERENCES

1. Amoils SP, Deist MB, Gous P, Amoils PM. Iatrogenic keratectasia after laser in situ keratomileusis for less than −4.0 to −7.0 diopters of myopia. J Cataract Refract Surg. 2000; 26:967–977. [PubMed: 10946186]
2. Binder PS, Lindstrom RL, Stulting RD, Donnenfeld E, Wu H, McDonnell P, Rabinowitz Y. Keratoconus and corneal ectasia after LASIK [letter]. J Cataract Refract Surg. 2005; 31:2035–2038. [PubMed: 16412891]
3. Krachmer JH, Feder RS, Belin MW. Keratoconus and related noninflammatory corneal thinning disorders. Surv Ophthalmol. 1984; 28:293–322. [PubMed: 6230745]
4. Randleman JB, Russell B, Ward MA, Thompson KP, Stulting RD. Risk factors and prognosis for corneal ectasia after LASIK. Ophthalmology. 2003; 110:267–275. [PubMed: 12578766]
5. Seiler T, Quurke AW. Iatrogenic keratectasia after LASIK in a case of forme fruste keratoconus. J Cataract Refract Surg. 1998; 24:1007–1009. [PubMed: 9682124]
6. Randleman JB, Woodward M, Lynn MJ, Stulting RD. Risk assessment for ectasia after corneal refractive surgery. Ophthalmology. 2008; 115:37–50. [PubMed: 17624434]
7. Kanellopoulos AJ. Collagen cross-linking in early keratoconus with riboflavin in a femtosecond laser-created pocket: initial clinical results. J Refract Surg. 2009; 25:1034–1037. [PubMed: 19731884]
8. Gaster RN, Caiado Canedo AL, Rabinowitz YS. Corneal collagen cross-linking for keratoconus and post-LASIK ectasia. Int Ophthalmol Clin. 2013; 53(1):79–90. [PubMed: 23221887]
9. Avitabile T, Franco L, Ortisi E, Castiglione F, Pulvirenti M, Torrisi B, Castiglione F, Reibaldi A. Keratoconus staging; a computer-assisted ultrabiomicroscopic method compared with videokeratographic analysis. Cornea. 2004; 23:655–660. [PubMed: 15448489]
10. Li X, Rabinowitz YS, Rasheed K, Yang H. Longitudinal study of the normal eyes in unilateral keratoconus patients. Ophthalmology. 2004; 111:440–446. [PubMed: 15019316]
11. Maguire LJ, Bourne WM. Corneal topography of early keratoconus. Am J Ophthalmol. 1989; 108:107–112. [PubMed: 2757091]
12. Rabinowitz YS, Rasheed K. KISA% index: a quantitative videokeratography algorithm embodying minimal topographic criteria for diagnosing keratoconus. J Cataract Refract Surg. 2000; 1999; 25:1327–1335. errata, 2000 26:480. [PubMed: 10511930]
13. Wilson SE, Lin DTC, Klyce SD. Corneal topography of keratoconus. Cornea. 1991; 10:2–8. [PubMed: 2019102]
14. Ambrósio R, Dawson DG, Salomão M, Guerra FP, Caiado ALC, Belin MW Jr. Corneal ectasia after LASIK despite low preoperative risk: tomographic and biomechanical findings in the unoperated, stable, fellow eye. J Refract Surg. 2010; 26:906–911. [PubMed: 20481412]
15. Klein SR, Epstein RJ, Randleman JB, Stulting RD. Corneal ectasia after laser in situ keratomileusis in patients without apparent preoperative risk factors. Cornea. 2006; 25:388–403. [PubMed: 16670474]
16. Reinstein DZ, Silverman RH, Sutton HFS, Coleman DJ. Very high-frequency ultrasound corneal analysis identifies anatomic correlates of optical complications of lamellar refractive surgery; anatomic diagnosis in lamellar surgery. Ophthalmology. 1999; 106:474–482. [PubMed: 10080202]
17. Huang D, Tang M, Shekhar R. Mathematical model of corneal surface smoothing after laser refractive surgery. Am J Ophthalmol. 2003; 135:267–278. [PubMed: 12614741]

18. Silverman RH, Urs R, RoyChoudhury A, Archer TJ, Gobbe M, Reinstein DZ. Epithelial remodeling as basis for machine-based identification of keratoconus. Invest Ophthalmol Vis Sci. 2014; 55:1580–1587. Available at:http://www.ncbi.nlm.nih.gov/pmc/articles/PMC3954156/pdf/i1552-5783-55-3-1580.pdf. [PubMed: 24557351]
19. Reinstein DZ, Archer TJ, Gobbe M. Corneal epithelial thickness profile in the diagnosis of keratoconus. J Refract Surg. 2009; 25:604–610. [PubMed: 19662917]
20. Kanellopoulos AJ, Aslanides IM, Asimellis G. Correlation between epithelial thickness in normal corneas, untreated ectatic corneas, and ectatic corneas previously treated with CXL; is overall epithelial thickness a very early ectasia prognostic factor? Clin Ophthalmol. 2012; 6:789–800. Available at:http://www.ncbi.nlm.nih.gov/pmc/articles/PMC3373227/pdf/opth-6-789.pdf. [PubMed: 22701079]
21. Li Y, Tan O, Brass R, Weiss JL, Huang D. Corneal epithelial thickness mapping by Fourier-domain optical coherence tomography in normal and keratoconic eyes. Ophthalmology. 2012; 119:2425–2433. Available at:http://www.ncbi.nlm.nih.gov/pmc/articles/PMC3514625/pdf/nihms389040.pdf. [PubMed: 22917888]
22. Rocha KM, Perez-Straziota CE, Stulting RD, Randleman JB. SD-OCT analysis of regional epithelial thickness profiles in keratoconus, postoperative corneal ectasia, and normal eyes. J Refract Surg. 2013; 29:173–179. errata, 234. [PubMed: 23446013]
23. Huang D, Swanson EA, Lin CP, Schuman JS, Stinson WG, Chang W, Hee MR, Flotte T, Gregory K, Puliafito CA, Fujimoto JG. Optical coherence tomography. Science. 1991; 254:1178–1181. [PubMed: 1957169]
24. Li Y, Meisler DM, Tang M, Lu ATH, Thakrar V, Reiser BJ, Huang D. Keratoconus diagnosis with optical coherence tomography pachymetry mapping. Ophthalmology. 2008; 115:2159–2166. [PubMed: 18977536]
25. Li Y, Shekhar R, Huang D. Corneal pachymetry mapping with high-speed optical coherence tomography. Ophthalmology. 2006; 113:792–799. e2. [PubMed: 16650675]
26. Li Y, Tang M, Zhang X, Salaroli CH, Ramos JL, Huang D. Pachymetric mapping with Fourier-domain optical coherence tomography. J Cataract Refract Surg. 2010; 36:826–831. [PubMed: 20457376]
27. Binder PS, Lindstrom RL, Stulting RD, Donnenfeld E, Wu H, McDonnell P, Rabinowitz Y. Keratoconus and corneal ectasia after LASIK. J Refract Surg. 2005; 21:749–752. [PubMed: 16329368]
28. Jafri B, Li X, Yang H, Rabinowitz YS. Higher order wavefront aberrations and topography in early and suspected keratoconus. J Refract Surg. 2007; 23:774–781. [PubMed: 17985796]
29. Lee BW, Jurkunas UV, Harissi-Dagher M, Poothullil AM, Tobaigy FM, Azar DT. Ectatic disorders associated with a claw-shaped pattern on corneal topography. Am J Ophthalmol. 2007; 144:154–156. [PubMed: 17601448]
30. Klyce SD. Chasing the suspect: keratoconus [editorial]. Br J Ophthalmol. 2009; 93:845–847. [PubMed: 19553507]
31. Westphal V, Rollins AM, Radhakrishnan S, Izatt JA. Correction of geometric and refractive image distortions in optical coherence tomography applying Fermat's principle. Opt Express. 2002; 10:397–404. Available at: http://www.opticsinfobase.org/oe/viewmedia.cfm?uri=oe-10-9-397&seq=0. [PubMed: 19436373]
32. Qin B, Chen S, Brass R, Li Y, Tang M, Zhang X, Wang X, Wang Q, Huang D. Keratoconus diagnosis with optical coherence tomography-based pachymetric scoring system. J Cataract Refract Surg. 2013; 39:1864–1871. [PubMed: 24427794]
33. Rabinowitz YS. Keratoconus. Surv Ophthalmol. 1998; 42:297–319. Available at: http://www.keratoconus.com/resources/Major+Review-Keratoconus.pdf. [PubMed: 9493273]
34. Reinstein DZ, Gobbe M, Archer TJ, Silverman RH, Coleman DJ. Epithelial, stromal, and total corneal thickness in keratoconus: three-dimensional display with Artemis very-high frequency digital ultrasound. J Refract Surg. 2010; 26:259–271. Available at:http://www.ncbi.nlm.nih.gov/pmc/articles/PMC3655809/pdf/nihms211821.pdf. [PubMed: 20415322]

35. Sandali O, El Sanharawi M, Temstet C, Hamiche T, Galan A, Ghouali W, Goemaere I, Basli E, Borderie V, Laroche L. Fourier-domain optical coherence tomography imaging in keratoconus; a corneal structural classification. Ophthalmology. 2013; 120:2403–2412. [PubMed: 23932599]
36. Waring GO III. Nomenclature for keratoconus suspects [opinion]. Refract Corneal Surg. 1993; 9:219–222. [PubMed: 8343441]
37. Bühren J, Kook D, Yoon G, Kohnen T. Detection of subclinical keratoconus by using corneal anterior and posterior surface aberrations and thickness spatial profiles. Invest Ophthalmol Vis Sci. 2010; 51:3424–3432. Available at: http://iovs.arvojournals.org/article.aspx?articleid=2126374. [PubMed: 20164452]
38. Maguire LJ, Lowry JC. Identifying progression of subclinical keratoconus by serial topography analysis. Am J Ophthalmol. 1991; 112:41–45. [PubMed: 1882920]
39. Saad A, Gatinel D. Evaluation of total and corneal wavefront high order aberrations for the detection of forme fruste keratoconus. Invest Ophthalmol Vis Sci. 2012; 53:2978–2992. Available at: http://iovs.arvojournals.org/article.aspx?articleid=2127924. [PubMed: 22427590]
40. Rabinowitz YS, Rasheed K, Yang H, Elashoff J. Accuracy of ultrasonic pachymetry and videokeratography in detecting keratoconus. J Cataract Refract Surg. 1998; 24:196–201. [PubMed: 9530594]
41. Pflugfelder SC, Liu Z, Feuer W, Verm A. Corneal thickness indices discriminate between keratoconus and contact lens-induced corneal thinning. Ophthalmology. 2002; 109:2336–2341. [PubMed: 12466180]
42. Ambrósio R, Caiado ALC, Guerra FP, Louzada R, Sinha Roy A, Luz A, Dupps WJ, Belin MW Jr. Novel pachymetric parameters based on corneal tomography for diagnosing keratoconus. J Refract Surg. 2011; 27:753–758. [PubMed: 21800785]
43. Saad A, Gatinel D. Topographic and tomographic properties of forme fruste keratoconus corneas. Invest Ophthalmol Vis Sci. 2010; 51:5546–5555. Available at: http://iovs.arvojournals.org/article.aspx?articleid=2126343. [PubMed: 20554609]
44. Temstet C, Sandali O, Bouheraoua N, Hamiche T, Galan A, El Sanharawi M, Basli E, Laroche L, Borderie V. Corneal epithelial thickness mapping using Fourier-domain optical coherence tomography for detection of form fruste keratoconus. J Cataract Refract Surg. 2015; 41:812–820. [PubMed: 25840306]
45. de Sanctis U, Aragno V, Dalmasso P, Brusasco L, Grignolo F. Diagnosis of subclinical keratoconus using posterior elevation measured with 2 different methods. Cornea. 2013; 32:911–915. [PubMed: 23572130]
46. de Sanctis U, Loiacono C, Richiardi L, Turco D, Mutani B, Grignolo FM. Sensitivity and specificity of posterior corneal elevation measured by Pentacam in discriminating keratoconus/subclinical keratoconus. Ophthalmology. 2008; 115:1534–1539. [PubMed: 18405974]
47. Muftuoglu O, Ayar O, Ozulken K, Ozyol E, Akinci A. Posterior corneal elevation and back difference corneal elevation in diagnosing forme fruste keratoconus in the fellow eyes of unilateral keratoconus patients. J Cataract Refract Surg. 2013; 39:1348–1357. [PubMed: 23820305]
48. Schlegel Z, Hoang-Xuan T, Gatinel D. Comparison of and correlation between anterior and posterior corneal elevation maps in normal eyes and keratoconus-suspect eyes. J Cataract Refract Surg. 2008; 34:789–795. [PubMed: 18471634]
49. Bühren J, Kühne C, Kohnen T. Defining subclinical keratoconus using corneal first-surface higher-order aberrations. Am J Ophthalmol. 2007; 143:381–389. [PubMed: 17317387]
50. Bühren J, Schäffeler T, Kohnen T. Validation of metrics for the detection of subclinical keratoconus in a new patient collective. J Cataract Refract Surg. 2014; 40:259–268. [PubMed: 24360499]
51. Shetty R, Matalia H, Srivatsa P, Ghosh A, Dupps WJ, Sinha Roy A Jr. A novel Zernike application to differentiate between three-dimensional corneal thickness of normal corneas and corneas with keratoconus. Am J Ophthalmol. 2015; 160:453–462. [PubMed: 26067190]
52. Arbelaez MC, Versaci F, Vestri G, Barboni P, Savini G. Use of a support vector machine for keratoconus and subclinical keratoconus detection by topographic and tomographic data. Ophthalmology. 2012; 119:2231–2238. [PubMed: 22892148]

53. Smadja D, Touboul D, Cohen A, Doveh E, Santhiago MR, Mello GR, Krueger RR, Colin J. Detection of subclinical keratoconus using an automated decision tree classification. Am J Ophthalmol. 2013; 156:237–246. [PubMed: 23746611]

Other Cited Material

A. Li, Y.; Tan, O.; Huang, D. Normal and Keratoconic Corneal Epithelial Thickness Mapping Using Fourier-Domain Optical Coherence Tomography. presented at the Proceedings of the SPEI: Medical Imaging 2011: Biomedical Applications in Molecular, Structural, and Functional Imaging; February 2011; Lake Buena Vista, Florida, USA.

B. [Accessed October 13, 2015] Center for Ophthalmic Optics and Lasers. Available at: http://www.coollab.net/#!resources/c43s

Biography

WHAT WAS KNOWN

- The epithelial PSD variable can be used to diagnose keratoconus.

WHAT THIS PAPER ADDS

- The epithelial PSD variable detected the epithelial thickness change in subclinical keratoconic eyes with high accuracy.
- The corneal thickness PSD variable might also be useful in the detection of early keratoconus.

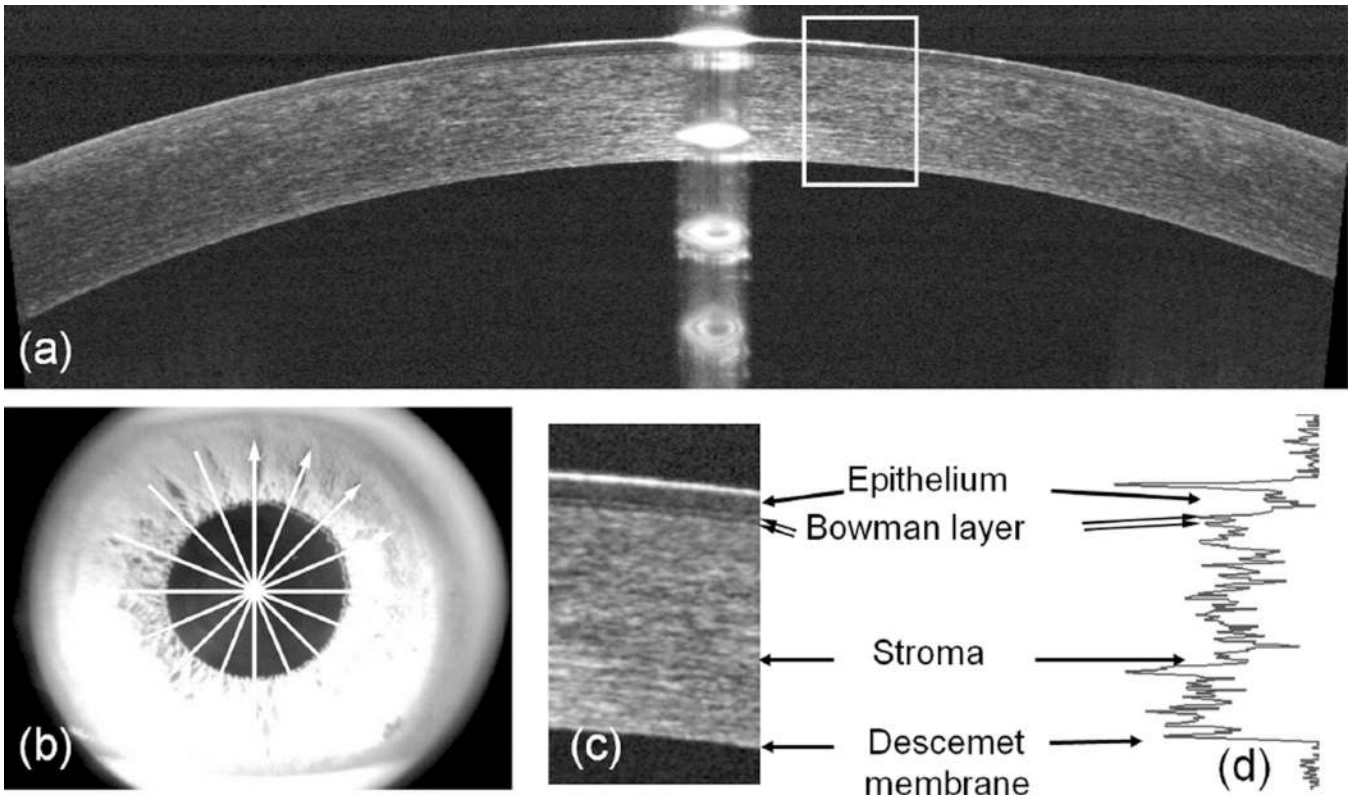

Figure 1.

a: Cross-sectional corneal OCT image (average of 5 repeated frames). *b*: The "Pchymetry +Pwr" scan pattern consisted of 8 radial scans. *c*: Magnified section of the OCT image. *d*: Corneal axial scan.

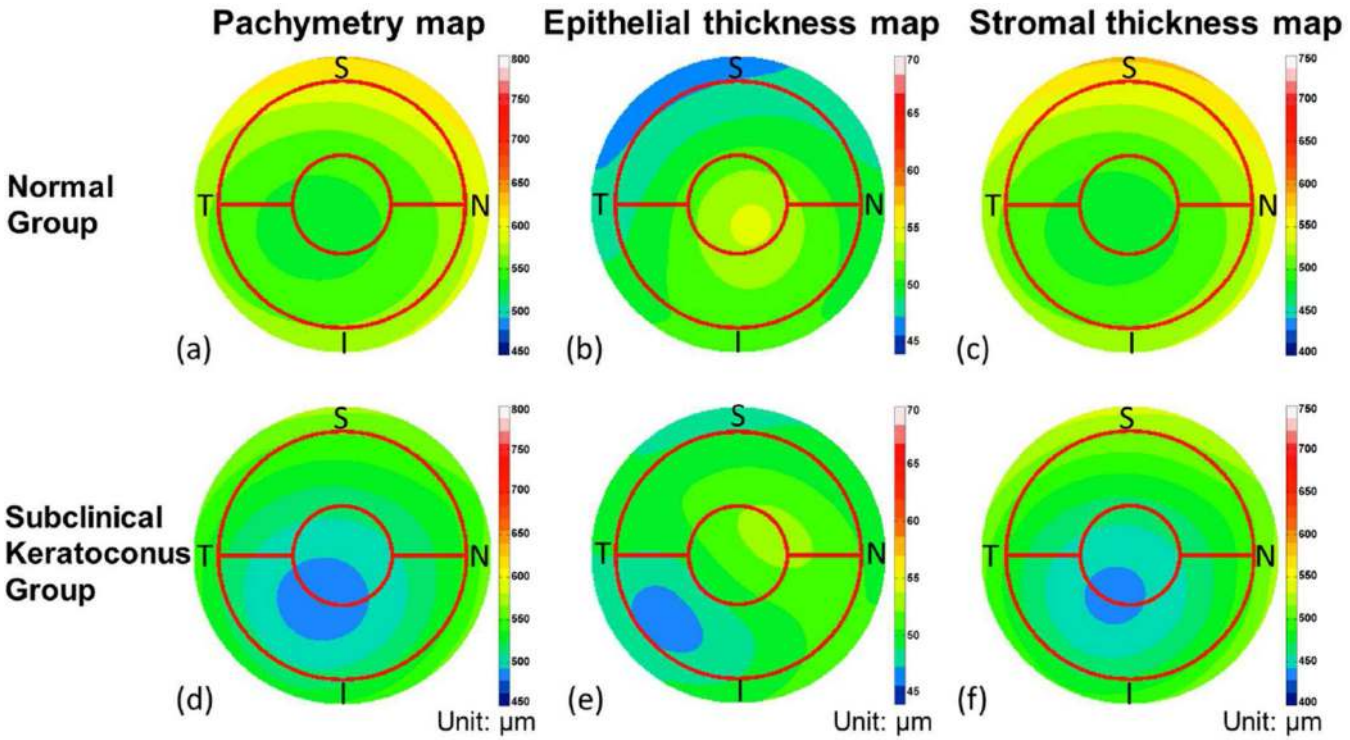

Figure 2.

Average pachymetric, corneal epithelial, and stromal thickness maps of normal (*a* to *c*) and subclinical keratoconus eyes (*d* to *f*). Maps of the left eyes that were included were mirrored before averaging. The red circles overlaid on the map had diameters of 2.0 mm and 5.0 mm. The color scale represents the thickness in microns (I = inferior; N = nasal; S = superior; T = temporal).

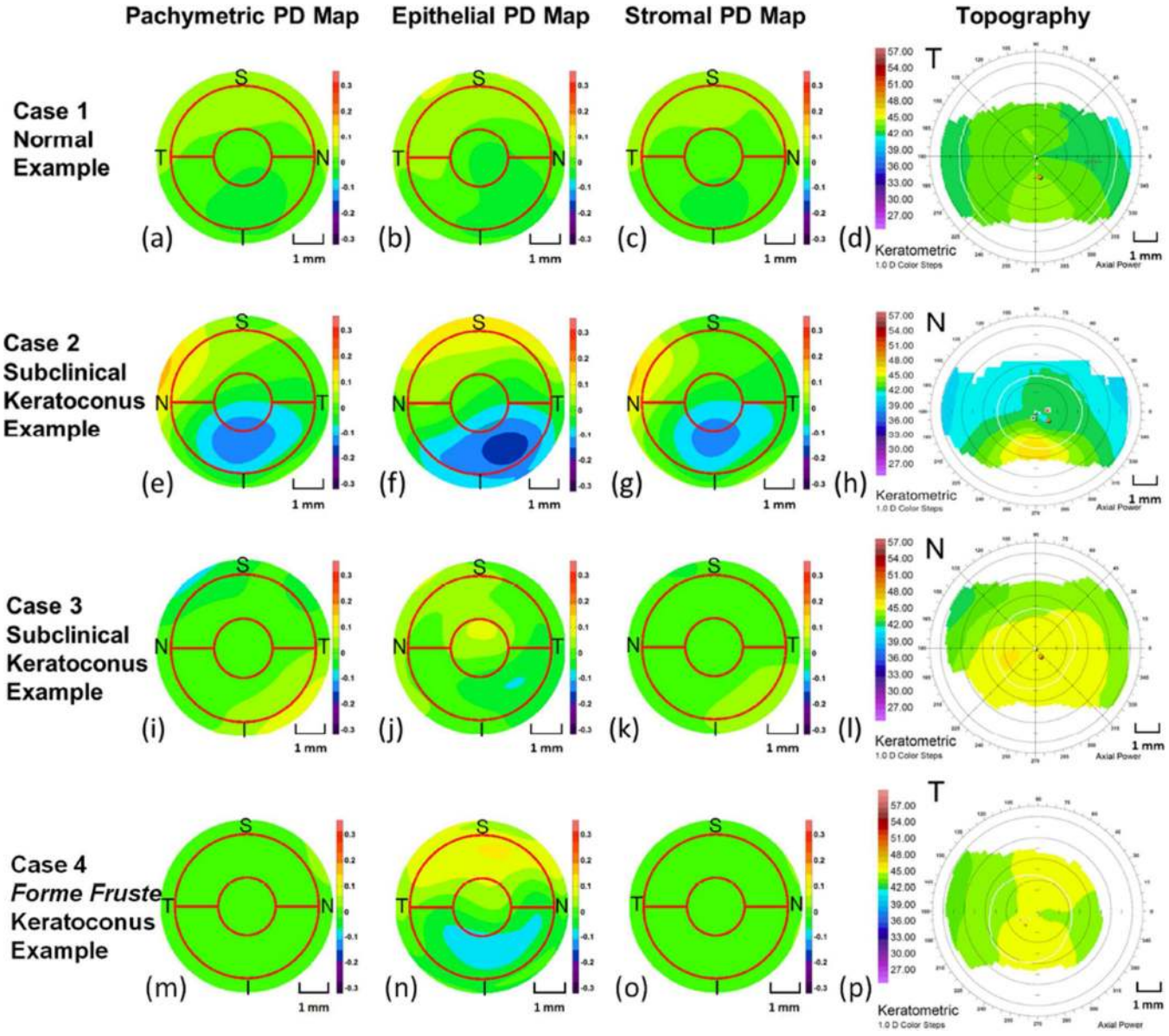

Figure 3.

Pachymetric, epithelial, and stromal pattern deviation maps and topography maps of 1 normal eye and 2 subclinical keratoconus eyes. The color scale of the pattern deviation maps has no units. The red circles overlaid on pattern deviation maps had diameters of 2.0 mm and 5.0 mm. Case 1 (*top row*) was a randomly chosen normal right eye of a 48-year-old woman. Her CDVA was 20/15. The topographic simulated K readings were 42.6 D and 43.7 D. The KISA% was 10.3%. All 3 PSD variables had normal values (pachymetric PSD_P = 0.010; epithelial PSD_E = 0.025; stromal PSD_S = 0.010). The pattern deviation maps (*a* to *c*) were relatively uniform. The topography map (*d*) had a normal appearance. Case 2 (*second row*) was a 24-year-old man with subclinical keratoconus in the left eye. His CDVA was 20/20. The simulated K readings were 41.6 D and 43.1 D. The KISA% was 41%. All 3 PSD variables exceeded cutoff values (PSD_P = 0.031; PSD_E = 0.092; PSD_S = 0.027). The pattern

deviation maps (*e* to *g*) showed apical thinning inferotemporally. The topography map showed asymmetric bowtie with skewed radial axis and inferior steepening. Case 3 (*third row*) was a 53-year-old woman with subclinical keratoconus in the left eye. Her CDVA was 20/15. The simulated K readings were 44.7 D and 45.5 D. The KISA% was 1.3%. The pachymetric and epithelial PSD variables were abnormal ($PSD_P = 0.020$; $PSD_E = 0.072$). The stromal PSD value appeared to be normal ($PSD_S = 0.017$). The epithelial pattern deviation map (*j*) showed apical thinning and surrounding thickening. The topography map showed inferior steepening. Case 4 (*bottom row*) was a 22-year-old man with forme fruste keratoconus in the right eye. His CDVA was 20/15. The simulated K readings were 44.4 D and 45.2 D. The KISA% was 9.0%. The epithelial PSD variable was abnormal ($PSD_E = 0.057$). The pachymetric and stromal PSD values were in the normal range ($PSD_P = 0.012$; $PSD_S = 0.010$). The epithelial pattern deviation map (*n*) showed epithelial thinning inferiorly and thickening superiorly. The topography map (*p*) appeared normal (I = inferior; N = nasal; PD = pattern deviation; S = superior; T = temporal).

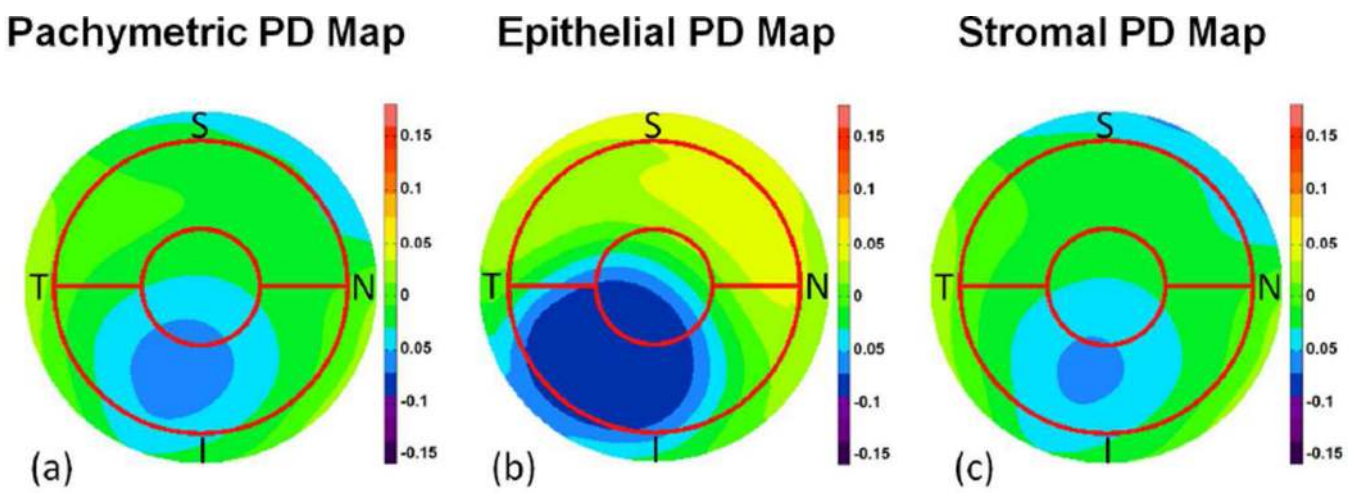

Figure 4.

Average pachymetric (*a*), corneal epithelial (*b*), and stromal (*c*) pattern deviation maps of subclinical keratoconic eyes. The color scale of pattern deviation maps has no units. The red circles overlaid on the map had diameters of 2.0 mm and 5.0 mm (I = inferior; N = nasal; PD = pattern deviation; S = superior; T = temporal).

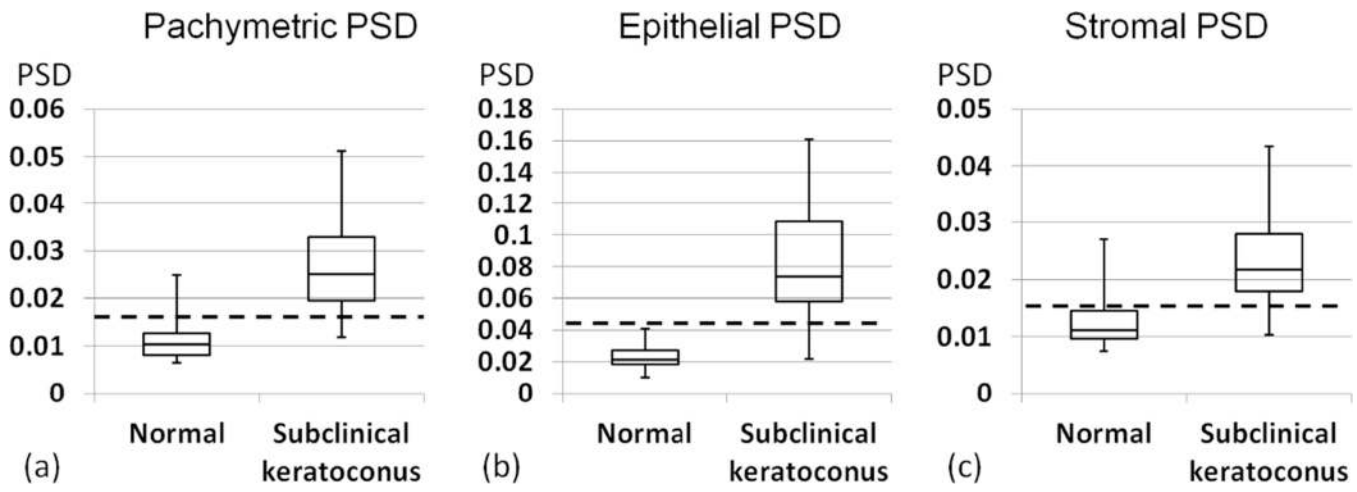

Figure 5.

Box-and-whisker plots of pachymetric, epithelial, and stromal PSD variables in normal and subclinical keratoconic eyes. The bottom and top of the box marks the first and third quartiles, the band inside the box is the median, and the whiskers represent the minimum and maximum of the data. The dashed lines mark the cutoff value of PSD variables (PSD = pattern standard deviation).

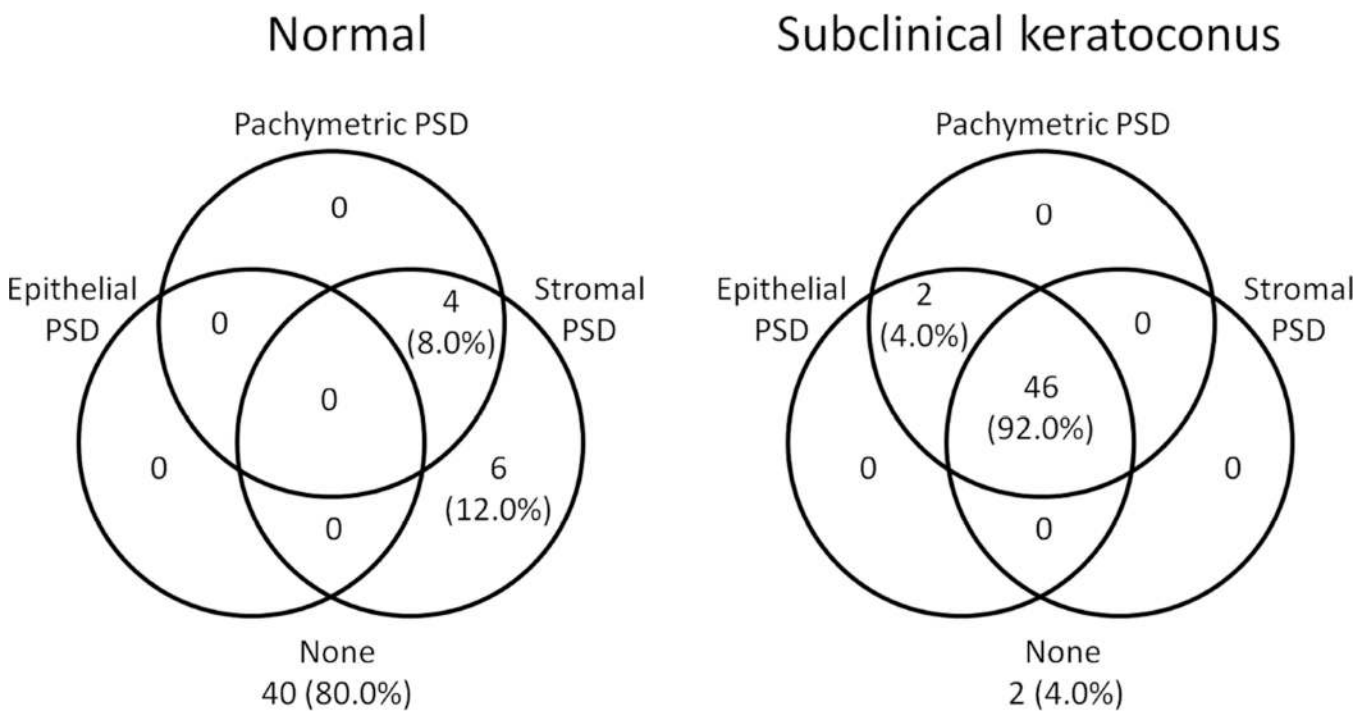

Figure 6.

Venn diagram showing the overlap between abnormal pachymetric, epithelial, and stromal PSD variables in normal eyes and subclinical keratoconus eyes. Abnormalities were detected by cutoff values listed in Table 3 (PSD = pattern standard deviation).

Table 1

Characteristics of normal eyes and eyes with subclinical keratoconus.

Group	n	Mean Steep K (D)	CDVA*		Mean Minimum Pachymetry (μm)	Mean Minimum Epithelial Thickness (μm)	Mean Minimum Stromal Thickness (μm)
			LogMAR	Equivalent Snellen			
Normal†	150	44.8 ±1.7	−0.07	20/18.6	529.9 ± 23.4	46.4 ± 3.8	476.0 ± 22.8
Subclinical KC†	50	45.1 ± 1.9	−0.05	20/19.0	482.6 ± 36.0	43.7 ± 5.4	434.7 ± 32.8
P value‡	–	.087	.033		<.001	.006	.053

CDVA = corrected distance visual acuity; K = keratometry; KC = keratoconus; n = number of eyes

*Cataract patients were excluded from CDVA calculation.

†Mean ± SD

‡One eye was randomly chosen for *t* tests if both eyes of a subject were involved in the study.

J Cataract Refract Surg. Author manuscript; available in PMC 2017 February 01.

Table 2

Descriptive statistics of OCT-based keratoconus diagnostic indices.

Group	Corneal PSD	Epithelial PSD	Stromal PSD	Pachymetric Map–Based KC Risk Score
Normal *	0.011 ± 0.004	0.022 ± 0.007	0.012 ± 0.004	1.7 ± 1.9
Subclinical KC *	0.026 ± 0.009	0.080 ± 0.030	0.023 ± 0.007	4.1 ± 3.0
P value †	<.001	<.001	.049	<.001

KC = keratoconus; PSD = pattern standard deviation

* Mean ± SD

† The 2-tailed *t* test compared the means of the normal group and the subclinical keratoconus group. The fellow eye was excluded from *t* tests to eliminate the correlation between the 2 eyes of a subject.

Table 3

Diagnostic accuracy of OCT-based keratoconus diagnostic indices.

Parameter	Pachymetric PSD	Epithelial PSD	Stromal PSD	KC Risk Score*
Criteria	>0.017	>0.041	>0.015	>4
Sensitivity	92.0	96.0	92.0	50.0
Specificity	92.0	100.0	80.0	90.0
AUC	0.941	0.985	0.924	0.735
AUC 95% CI	0.88, 0.98	0.94, 1.00	0.85, 0.97	0.63, 0.82

AUC = area under the receiver operating characteristic curve; CI = confidence interval; KC = keratoconus; PSD = pattern standard deviation

*Pachymetric map based

Table 4

Repeatability of PSD variables.

	Normal		Subclinical KC	
Diagnostic Parameter	**ICC**	**SD**	**ICC**	**SD**
Pachymetric PSD	0.836	0.0018	0.92	0.0021
Epithelial PSD	0.932	0.0024	0.982	0.0033
Stromal PSD	0.838	0.002	0.90	0.0022

ICC = intraclass correlation; KC = keratoconus; PSD = pattern standard deviation; SD = pooled standard deviation